Improving mechanical robustness of ultralow-*k* SiOCH plasma enhanced chemical vapor deposition glasses by controlled porogen decomposition prior to UV-hardening

A. M. Urbanowicz,[1,2,a)] K. Vanstreels,[2] P. Verdonck,[2] D. Shamiryan,[2] S. De Gendt,[1,2] and M. R. Baklanov[2]
[1]*Department of Chemistry, Katholieke Universiteit Leuven, B-3000 Leuven, Belgium*
[2]*IMEC, B-3001 Heverlee, Belgium*

(Received 15 March 2010; accepted 10 April 2010; published online 27 May 2010)

We report a new curing procedure of a plasma enhanced chemical vapor deposited SiCOH glasses for interlayer dielectric applications in microelectronic. It is demonstrated that SiOCH glasses with improved mechanical properties and ultralow dielectric constant can be obtained by controlled decomposition of the porogen molecules used to create nanoscale pores, prior to the UV-hardening step. The Young's modulus (YM) of conventional SiOCH-based glasses with 32% open porosity hardened with porogen is 4.6 GPa, this value is shown to increase up to 5.2 GPa with even 46% open porosity, when the glasses are hardened after porogen removal. This increase in porosity is accompanied by significant reduction in the dielectric constant from 2.3 to 1.8. The increased YM is related to an enhanced molecular-bridging mechanism when film is hardened without porogen that was explained on the base of percolation of rigidity theory and random network concepts.
 [doi:10.1063/1.3428958]

I. INTRODUCTION

Nanoporous organosilica glasses (OSG) are used for emerging optical, electronic, and biological technologies. Those materials have found various applications from biological scaffolds over catalysis and hydrogen storage to microelectronic devices. One particular example of OSG application is microelectronics. The nanometre-scale porosity is deliberately introduced to reduce the dielectric constant (k), making OSG suitable for use as insulating layers around thin metal lines that carry electrical signals in microelectronic devices. However, incorporating the porosity also degrades the mechanical properties of OSG, presenting a challenge for their integration into ultralarge-scale microelectronic devices.[1–4] Microelectronic industry uses two different deposition approaches of the porous OSG: spin-on (from liquid solutions/gels) and plasma enhanced chemical vapor deposition (PECVD). The spin-on approach is well explored,[5] the OSG with wide range of porosity up to 99% has been achieved using various ways to introduce porosity, e.g., silica-particles nanotemplating,[19] sacrificial-porogen method, or templated sol-gel polymerization of bridged silsesquioxane precursors.[6] In contrast, PECVD glasses are less explored but presently they are more popular in microelectronic due to the better compatibility with technology requirements.[7–10] The introduction of porosity into PECVD ultralow-*k* OSG is mainly realized by using sacrificial porogens.[11] The matrix material is codeposited with porogen molecules. Precursors of the matrix materials are alkylsilanes, the porogen molecules are usually cyclic hydrocarbons.[9] To create porosity, the porogen is removed by UV-assisted-thermal curing process (hardening step) in which a formation of the reinforced Si—O—Si network occurs simultaneously.[12] However, not all porogen is removed during the curing, it is partially converted by UV-light into nonvolatile graphitized-carbon residues [porogen residue (PR)]. Therefore, such prepared OSG can be considered as a dual-phase system containing a rigid organosilica skeleton and soft PR. The total Young's modulus (YM) of such a dual-phase OSG is expected to be smaller than that of single-phase OSG containing mostly rigid Si—O—Si links and terminal organic groups (Si—CH_3). In this work we discuss PR detection using spectroscopic ellipsometry (SE). We argue that the conventionally fabricated PECVD glasses with ultralow *k*-value (highly porous) contain PR in contrast to spin-on fabricated glasses using PR-free approach that results in higher YM and better electrical characteristic of the spin-on films. We propose the new approach of fabrication PR-free PECVD films by selective porogen removal prior to UV-assisted hardening step. This approach is demonstrated to be beneficial for both low-*k* value and mechanical properties of the dielectric film.

II. EXPERIMENTAL

A. Materials and experimental procedure

The organosilica matrix was codeposited with organic porogen by PECVD on 300 mm Si wafers at 300 °C. The OSGs with thicknesses of 65, 120, and 190 nm were obtained as described in literature.[33] Next the films were treated with four combinations of the H_2 after-glow treatment (H_2-AFT) and UV-curing: UV, H_2-AFT, H_2-AFT+UV, UV +H_2-AFT. The H_2-AFT treatments were performed at a wafer temperature of 280 °C using 350 s of the He/H_2 20:1 downstream microwave plasma treatment in a 300 mm asher from LAM research. The He was used to dilute H_2 and in-

a)Author to whom correspondence should be addressed. Tel.: +32 16281469. FAX: +32 16281214. Electronic mail: urbano@imec.be.

crease its dissociation efficiency. The pure H_2 has similar effect on SOG films except that the depth of porogen removal is smaller due to lower H radical concentration. The effect of UV-radiation from plasma area was canceled by special design of the chamber. The UV-curing was performed in nitrogen ambient at temperature close to 430 °C. The new curing procedure was performed using a narrow-band 172 nm UV-source.[33] In order to compare porogen removal efficiency of H_2-AFT with the different wavelengths of UV irradiation, an additional experiment with a broadband UV-source with the wavelengths higher than 200 nm was performed.

B. Instrumentation

The surface hydrophobic properties before and after the plasma treatments were evaluated using water contact angle measurements (WCA). Optical properties were determined by SE in the spectral range of 150 to 895 nm at an incidence angle of 70º using Aleris SE from KlaTencor. The results were fitted by a single and a double layer optical model using the Marquardt–Levenberg algorithm. The optical models were constructed as described in the literature.[16] The depth of modification and the optical properties of 190 nm films were estimated using a double layer SE model. The bottom layer was assumed to have optical properties of the as deposited film, while the optical characteristics of the top modified layer were determined by fitting. The mass change related to plasma treatments was measured by mass balance metrology on 300 mm wafers (Metrix: Mentor SF3). The open porosity and pore size distributions (PSDs) were evaluated using ellipsometric porosimetry (EP).[13] Mechanical properties, YM and hardness of the low-*k* dielectric films were measured using a Nanoindenter XP® system (MTS Systems Corporation) with a dynamic contact module and a continuous stiffness measurement option under the constant strain rate condition. A standard three-sided pyramid diamond indenter tip (Berkovich) was used for the indentation experiments. As the indenter tip is pressed into each sample, both depth of penetration (h) and the applied load (P) are monitored. The YM values of thin OSGs could be influenced by Si substrate effect. The Si substrate effect might vary depending on film thickness. In order to exclude potential error in YM values the film with different thicknesses are investigated in this study. The more detailed discussion about nanoindentation (NI) measurement of thin porous OSGs is reported in literature.[29,30]

III. RESULTS AND DISCUSSION

The effect of the PR on optical, chemical, and mechanical properties of PECVD deposited SOG is a subject of intensive research.[14–17] It was shown that PR increases the extinction coefficient of OSG in the UV-range.[16,18] Figure 1 reflects extinction of PECVD and spin-on[19] OSG's with $k=2.3$ and PECVD deposited matrix material (without porogen) and SiO_2 films. One can see that the extinction coefficient of spin-on film and PECVD matrix material deposited without porogen are more close to SiO_2. The PECVD glass prepared by standard codeposition of organosilica matrix and

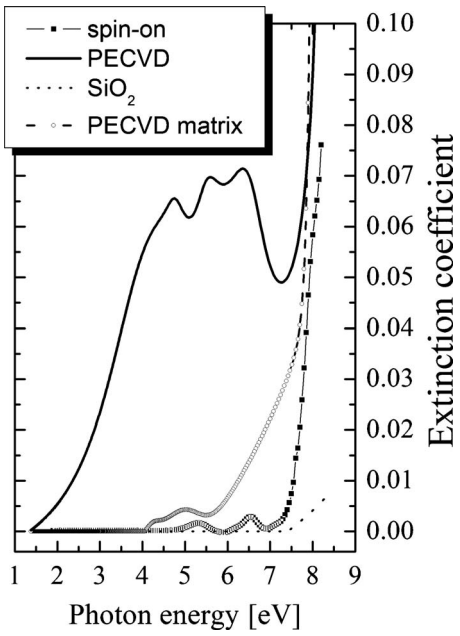

FIG. 1. Extinction coefficient (as measured by UV SE) of SiO_2 deposited by PECVD using SiH_4 as a precursor, PECVD matrix material, standard spin-on nanoclustered silica, and PECVD low-*k* films.

porogen followed by UV-curing show significantly higher extinction than the rest of the films. In addition, the low energy shoulder with a maximum at 4.5 eV in the extinction coefficient reflects the presence of sp^2 hybridized carbon (PR).[14,20]

Although porogen is needed to introduce porosity in PECVD glasses, the PR has a negative impact on the fundamental properties of OSG's and their industrial processing compatibility. The presence of PR with conjugated C═C bonds increases the leakage current and decreases the breakdown voltage of these materials (—C═C—C═C—C═C is a classical conducting polymer).[21,22] Moreover, organic-free nanoclustered silica OSG (Ref. 19) deposited by spin-on shows higher YM of 6.54 GPa than OSG deposited by PECVD that has YM of 4.6 GPa for the same *k*-value of 2.3 as shown in Table I (similar porosity level). This indicates that PR-phase present in PECVD glass might be the reason of its lower YM than spin-on glass. Furthermore, the industrial processing, such as a photomask removal from PECVD OSG also removes PR from the latter that results in porosity increase and subsequent degradation of mechanical properties.[15,16] Therefore, development of a new curing approach allowing preparation of PR-free and a mechanically robust PECVD ultralow-*k* films is the main goal of this work.

In order to explain higher mechanical robustness of spin-on OSG in comparison with PECVD ones, we investigated their fabrication steps with emphasis on the role of organic residues. There are two differences out of many others between spin-on organosilica particles nanotemplating and PECVD fabrication approaches of OSG that are important for our consideration. The first difference is that the spin-on glass is normally deposited at room temperatures, while the PECVD glass at temperatures typically higher than 180 °C (300 °C in our case).[9,23] The higher deposition temperature of PECVD glass results in partial cross-linking of

TABLE I. Comparison of the properties of conventionally UV-cured with H_2-AFT+UV cured OSGs. The used abbreviations mean: Th_{init} (initial thickness), Th_{final} (final thickness), WCA (water contact angle), MPR (meant pore radii), H (hardness). The conventional spin-on film characteristics prepared by nanoclustering of silica nanoparticles were added for comparison.

Th_{init} (nm)	H_2-AFT (s)	UV (s)	Th_{final} (nm)	WCA (°)	$k_{100\ kHz}$	YM (GPa)	H (GPa)	Open porosity (%)	$RI_{632\ nm}$	MPR (nm)
65	350	83	58	92.0	1.79	5.82 ± 0.82	0.63 ± 0.07	46	1.223	1.5
120	350	166	105	90.8	1.87	5.46 ± 0.51	0.60 ± 0.08	46	1.228	1.5
190	350	249	154*	87.9	2.24	7.08 ± 0.62	0.77 ± 0.06	N/A	N/A	N/A
240	$2 \times 350^{+}$	333	191	78.8	2.30	8.38 ± 0.52	0.80 ± 0.08	43	1.250	1.4
600	$5 \times 350^{+}$	835	481	67.4	2.60	9.50 ± 0.61	1.00 ± 0.05	41	1.266	1.4
67	···	83	59	93.3	2.26	5.30 ± 0.42	0.49 ± 0.03	32	1.371	1.0
190	···	249	180	92.9	2.30	4.48 ± 0.16	0.39 ± 0.03	32	1.373	0.9
600	···	835	498	91.0	2.30	4.61 ± 0.32	0.57 ± 0.08	32	1.375	1.0
600	···	1800	462	57.1	2.49	5.72 ± 0.41	0.69 ± 0.09	30	1.408	1.0
140		Spin-on film		91.0	2.30	6.54 ± 0.77	0.80 ± 0.08	32	1.277	1.0

organic phase with film skeleton making it more difficult to remove. The second difference is that the spin-on glasses contain low amount of organics that are easily removed during thermal annealing (aging process), where the prehardening of Si—O—Si matrix occurs simultaneously. Moreover, UV-curing spin-on occurs in a (or alternatively e-beam curing or thermal curing) separate process step.[24] On the contrary, the PECVD approach realizes the final film hardening and the organic porogen removal in one UV-curing process that results in PR-creation.[16] Therefore, a possible solution to avoid PR-creation (which has negative effect on YM) is to remove the organic part (porogen) from the PECVD film matrix before the regular UV-curing, similar to the spin-on deposition approach. The PECVD deposition process occurs at sufficiently high temperature of 300 °C, so we can assume that similar phenomena occur as in aging process of spin-on films. The porogen agglomeration in the film should occur already during the film deposition. Therefore, the matrix should be sufficiently stiff (should not collapse) to allow porogen removal prior to regular UV-curing.

A. Selective porogen removal

One of the biggest challenges of porogen removal from PECVD OSG is selectivity. The removal of organic porogen should occur without modification of organosilica skeleton. The skeleton modification may lead to unwanted densification or hydrophilization of the OSG. For instance, the porogen removal by only thermal annealing requires temperatures higher than 350 °C that also leads to PR creation and skeleton cross-linking that results in OSG densification.[17] This is due to porogen thermodissociation temperature that is higher than temperature required for skeleton cross-linking.[17] Therefore, the porogen removal has to be realized in lower temperatures than 350 °C. One possible way to realize selective porogen removal is annealing the OSGs at 280 °C in H_2-based plasma afterglow treatment (H_2-AFT).[15,16] This process is similar to zero damage photoresist mask removal process reported elsewhere.[25,26] The organic photomasks containing C—C, C=C, and C—H bonds can be selectively removed from Si—CH_3-bond containing SiOCH low-*k* dielectrics, without any Si—CH_3 bonds scission.[15] Normally, the Si—CH_3 bonds scission leads to their replacement with Si—OH bonds and subsequent hydrophilization of OSG that results in drastic increase of *k*-value (k_{H_2O} is around 80 at 100 kHz).[1] The PR or the porogen also contain C=C and C—C bonds or C—H bonds, therefore, should be also selectively removed from low-*k* film matrix. In order to demonstrate this, we studied the effects of 350 s H_2-AFT at 280 °C and UV treatments at 350 °C on as-deposited matrix-porogen PECVD films of 60 nm. PECVD low-*k* films remain hydrophobic after H_2-AFT at 280 °C and UV treatments at 350°. The WCA with surfaces for all the films were approximately 90° (see Table I). The thickness loss and organic removal efficiency was evaluated by UV-SE. Less than 1% of thickness loss was measured for H_2-AFT.

B. Porogen and PR detection by UV-SE

Another challenge is related to quantitative evaluation of PR content in OSG matrix. Their quantitative evaluation cannot be performed by Fourier transform infrared (FTIR) spectroscopy that has a very limited sensitivity to PR because of nonpolar nature of C—Cand C=C bonds.[27] Therefore, quantitative detection of PR might be possible by Raman spectroscopy[21] but this metrology sometimes is challenging because of overlap of PR related absorption and photoinduced luminescence. Another problem is that low-*k* films can degrade under laser radiation used for generation of the scattering light. For this reason we used a nondirect method, UV SE (Refs. 14 and 16). Figure 2 shows the optical properties of the as deposited matrix-porogen film, the H_2-AFT and the UV-cured film.

The extinction coefficient of the as deposited film (with porogen) is the highest due to the highest porogen content. The H_2-AFT treatment results in complete removal of the porogen and PR and the final absorption becomes similar to the UV spectra of the low-*k* matrix material as shown in Fig. 1.[14] On the contrary, the standard UV-curing processes using narrow band (~172 nm) or broadband (>200 nm) UV-source results in the PR creation that is reflected in increased extinction coefficient (Fig. 2). Furthermore, the relative changes in refractive indices of the as deposited film and treated ones reflect to the porosity increase [the pore volume has refractive index (RI) of air close to 1]. The H_2-AFT treatments result in the highest RI reduction due to the po-

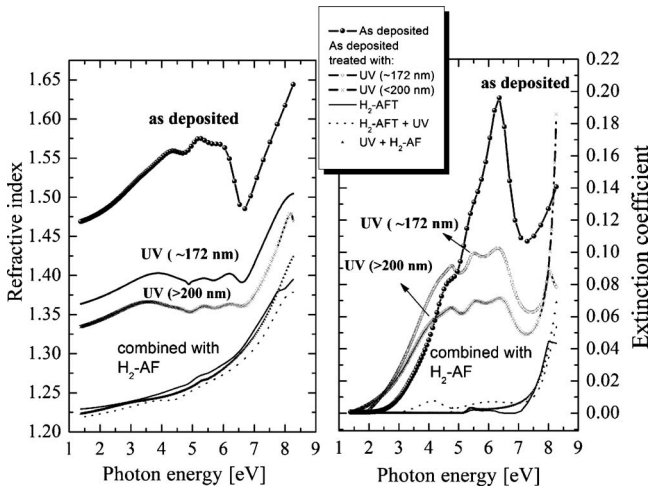

FIG. 2. Optical properties of differently prepared OSG as measured by UV-SE: as deposited film (matrix-porogen); as deposited matrix-porogen films cured with narrowband UV-light wavelength of 172 nm and broad band UV with wavelengths higher than 200 nm, H_2-AFT and two combined H_2-AFT, and 172 nm UV cures.

rosity increase caused by enhanced porogen removal. In order to estimate the amount of the organic residues, we used mass balance metrology. We measured the mass loss of 300 mm wafers with 60 nm films treated with the H_2-AFT and/or 172 nm UV. The results show that the conventional 172 nm UV-curing process leaves approximately 46% more mass in comparison to the H_2-AFT treatments. The results agree with the UV-SE data, that is less extinction corresponding to higher mass loss.

C. Mechanism of porogen removal

It is important to understand the mechanism of removal of the porogens in H_2-AFT. We propose that the porogen removal mechanism at high temperatures (around 300 °C) is similar to the photomask removal mechanism in H_2-AFT plasma[25] as shown in Fig. 3.

Hydrogen atoms promote dissociation of the high mass porogen chains render generation of volatile short chain alkyl molecules. One limiting factor for porogen removal depth is the penetration depth of the H radicals into porous low-*k*. The penetration depth of the H radicals is limited by their loss in low-*k* pores as a result of recombination on the low-*k* pore walls or chemical reaction with porogen or PR. The time dependent depth of penetration of H radicals for

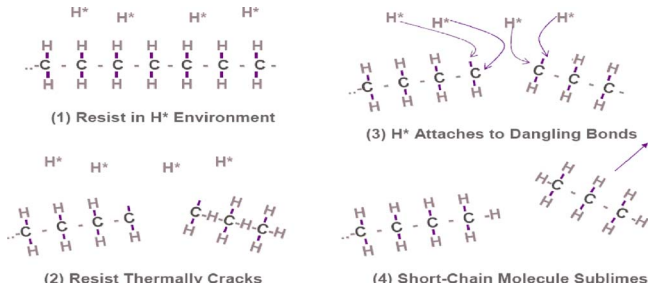

FIG. 3. (Color online) Schematic sketch of possible organic polymer removal mechanism by annealing in hydrogen after-glow atmosphere (Ref. 25).

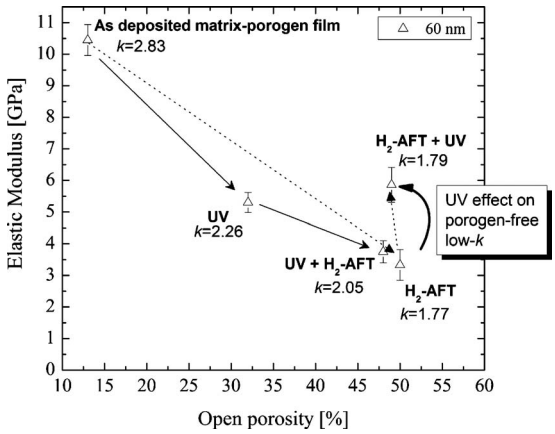

FIG. 4. YM as measured by NI vs open porosity as measured by EP. The *k*-values for all conditions were measured by Hg-probe at 100 kHz.

different low-*k* films was reported in literature.[16] It was found that it saturates logarithmically with time. In order to determine the depth of H radicals' penetration we treated the as deposited matrix-porogen film of 190 nm time of 350 s of H_2-AFT. Next, we measured the thickness of the porogen depleted layer by UV-SE using double-layer SE model. The depth of porogen removal was determined to be about 160 nm after 350 s of H_2-AFT. Therefore the thickness limit to achieve the uniform films using a subsequent H_2-AFT and UV-curing is about 160 nm. A thicker film fabrication should involve sequential film deposition combined with H_2-AFT curing. The UV curing should be then performed as a last step due to much higher penetration depth of UV-light (>172 nm) that is defined by Lambert-Beer law as compared to H radicals that is defined by diffusion-recombination of H-atoms on pore walls.

D. Effect of porogen and PRs on mechanical properties of low-*k* films

In order to study the effect of porogen or PR on mechanical properties, the YM and open porosity were measured such as: the as deposited film, the UV-treated (standard) film, and the films after combined H_2-AFT and UV treatments. The mechanical properties of the low-*k* films were evaluated using NI.[28] Since the film thicknesses were relatively small, a relative YM comparison of different OSGs with similar thickness was still possible.[29,30] Figure 4 shows YM versus open porosity and *k*-values. The drop in YM and increase in the open porosity after all the treatments is due to the porogen or the PR removal. As we reported previously the H_2-AFT of conventionally UV-cured film (UV +H_2-AFT) results in the porosity increase, *k*-value decrease and a reduction in mechanical properties. Those changes were due to the PR removal after UV.[15,16] This observation is indicated by the dashed arrows in Fig. 4. However, when the porogen is removed by the H_2-AFT prior to the UV-curing (H_2-AFT+UV) YM of the obtained film exceeds that of the conventionally UV-cured film. The latter observation is indicated by the dotted arrows.

We propose that the porogen removal prior to the UV-curing prevents a cross-linking of the porogen inside the

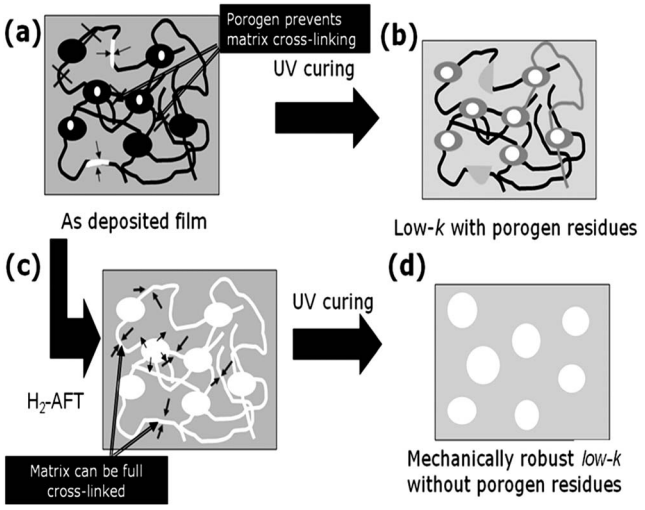

FIG. 5. Sketch of the simplified multiphase structure of PECVD material after: (a) deposition, (b) conventional UV-curing, (c) H_2-AFT treatment, and (d) UV-curing when porogen was removed by H_2-AFT. Areas with colors white, light gray, and black denote air, organosilica skeleton and porogen, respectively. Dark gray on picture (b) represents PRs.

SiOC:H skeleton. Therefore, the subsequent creation of the PR inside the low-*k* film skeleton is avoided. Moreover, the cross-linkage of the mechanically strong SiOC:H skeleton is not limited by the presence of organic PR as shown in Fig. 5. Therefore, much stronger Si—O bonds are created in the SiOCH skeleton in the absence of porogen. The Si—O links significantly improve YM of the film.

The PSD measurements (Fig. 6) agree with the sketch as shown in Fig. 5. The as deposited OSG is micro porous [Fig. 5(a)] and it has 13% of open porosity (Fig. 4). After the conventional UV-curing the porosity increases and the pores become larger. However, the pore radius of the conventionally UV-cured OSG is partly defined by the presence of PR on the pore walls [Fig. 5(b)]. This is clearly reflected in the enlarged pores after the PR removal by H_2-AFT. The PSD-measurement of the H_2-AFT treated PECVD films reveals that, PSD of the matrix contains both: micropores and mesopores [Fig. 5(c)]. When PR-free matrix is exposed to UV

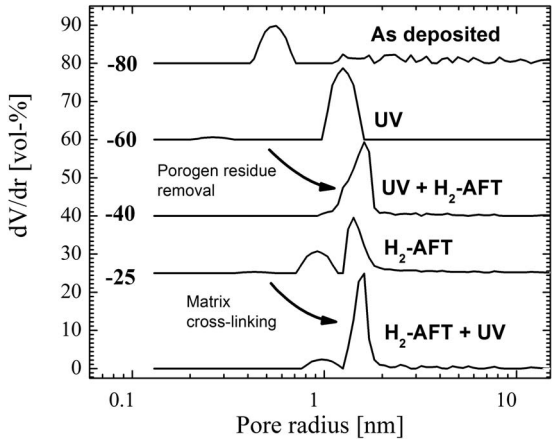

FIG. 6. PSD of the as deposited and the treated PECVD OSGs as measured by EP. The PSD were calculated from the desorption branches. Distributions have been shifted vertically for clarity.

light the micropores disappear due to the creation of additional cross-links (SiOCH matrix densification), and as a result the OSG becomes mesoporous.

E. Fabrication of the films with variable thicknesses

In order to confirm our hypothesis we cured the porogen-free glasses with variable thicknesses and compared their properties to the conventional OSGs cured with porogen. The as deposited films with thicknesses of 65, 120, and 190 nm, 2×120 nm and 5×120 nm were prepared using subsequent H_2-AFT and 172 nm UV-cure. The 2×120 nm and 5×120 nm OSGs were prepared by repeated PECVD of 120 nm films combined with the subsequent 350 s H_2-AFT. The basic properties of the obtained OSGs are reported in Table I. Two films of 58 and 105 nm, uniform from top to bottom, were obtained by subsequent H_2-AFT and UV-curing. The open porosity and the mean pore radii of 58 and 105 nm uniform OSGs were measured by EP. Both glasses have 46% of porosity and mean pore radii of 1.5 nm. The YM were 5.82 ± 0.82 GPa for the 58 nm glass and 5.46 ± 0.51 GPa for the 105 nm glass. In the case of the 190 nm film, the porogen was only partly removed due to the limited penetration of H-atoms to about 160 nm. The subsequent UV-light irradiation of 190 nm film results in creation of a bilayer OSG. Presumably, the transport of decomposed porogen fragments induced by UV-light resulted in increased film shrinkage as compared to the thinner films (enhanced cross-linkage of the SiOCH matrix). We additionally investigated the multilayered OSGs. The optical properties of those glasses as measured by UV-SE were fitted with a good accuracy using a single layer ellipsometric model. Therefore, the 2×120 nm and 5×120 nm have homogeneous optical properties; this indicates bulk uniformity. The OSGs were cured with the same times as porogen containing ones with the same thickness. The results clearly show (Table I) that the same UV-curing time results in much higher improvement of YM and H of porogen-free films. Moreover, the extended UV-curing time to 1800 s of porogen containing 600 nm OSG results in significantly lower YM and hardness than 835 s UV-cured porogen-free OSG. It is also important to mention that longer UV-cure times lead to hydrophilization due to photodissociation of Si—CH_3 groups from OSG and a subsequent moisture absorption from ambient.[31–33] The latter phenomenon results in slightly higher *k*-values and lower WCA of thicker porogen-free OSG since UV-curing time was longer. This effect is less pronounced for porogen containing OSG since decomposed organic porogen fragments such as CH_x groups can passivate dangling bonds created as result of Si—CH_3 bond scission.

F. Mechanism of mechanical properties improvement

Extraordinary mechanical properties of the H_2-AFT and UV treated films can be reasonably interpreted within the framework of the continuous random network theory and percolation of rigidity concepts first developed by Phillips[34] and expanded upon by Thorpe.[35] The percolation of rigidity defines a compositional point in a network where the system transitions from an underconstrained nonrigid state to an

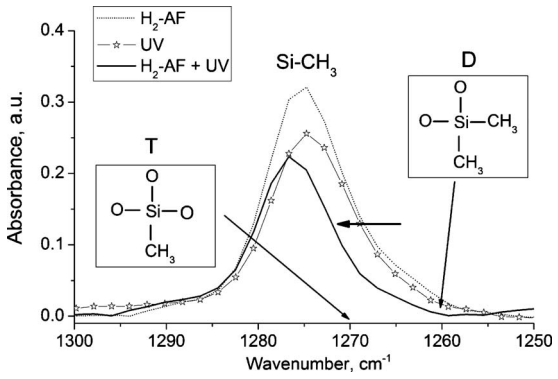

FIG. 7. The infrared absorption (as measured by FTIR) of terminal Si—CH_3 groups from the 60 nm OSGs treated with: 172 nm UV, H_2-AFT and subsequent H_2-AFT and 172 nm UV.

overconstrained rigid state. Systems above the percolation threshold would thus be expected to have superior mechanical properties as compared to those below the threshold, owing to the increased structural constraints. The key parameter in this analysis is the *average connectivity number* ⟨r⟩. The connectivity number is the average number of bonds per network forming atom. Network forming atoms have two or more bonds to other network forming atoms, and atoms having only one bond, such as hydrogen, do not contribute to the network and are not counted in the analysis. Dohler *et al.*[36] determined that the percolation of rigidity occurs at an average connectivity number of 2.4 for solids in which all atoms are able to form two or more bonds. This connectivity number of 2.4 for SiOCH materials is when only T-groups (O≡Si—CH_3) are present in the structural composition of the low-*k* film.[7] This is the case of our films as evidenced by FTIR data (Fig. 7).

The important difference is the shift in the Si—CH_3 absorption band (1250–1300 cm^{-1}) of H_2-AFT+UV treated film. This band can vary in position based upon the degree of oxidation of Si atom, with increasing oxidation shifting the band to higher wavenumbers.[37] The three most basic possibilities for the configuration are designed as "M" (~1250 cm^{-1}), "D" (~1260 cm^{-1}), "T" (~1270 cm^{-1}), reflecting either monosubstitution, disubstitution, or trisubstitution of the silicon atom by oxygen.[7,37] Therefore, for the H_2-AFT+UV treated glass, the shift in Si—CH_3 absorption band could be explained by the presence of mainly a T-rich structure, indicating the incursion of more oxygen into the OSG and potential cross-linking.

IV. CONCLUSION

In a summary, we demonstrated that porogen present during UV-curing of PECVD deposited OSG deteriorate its SiOCH matrix cross-linking, and that results in the reduced mechanical properties of the final film. We propose an improved fabrication procedure of enhanced chemical vapor deposited (PECVD) low-*k* films. The new procedure is performed by conventional UV-curing of PECVD film skeleton when the porogen is already completely removed. The removal of the organic porogen without Si—CH_3 bonds scission is found to be possible by annealing of the low-*k* film in a H_2-based plasma afterglow. The effective depth of the porogen removal depends on the penetration depth of the active H radicals into the porous SiOCH matrix and it is found to be approximately 160 nm. The proposed method allows us to obtain PR-free low-*k* films with variable thicknesses. The obtained films demonstrate extraordinary high YM of 5–9.5 GPa for open porosity in the range of 41%–46%, *k*-value of 1.8–2.6. The extraordinary mechanical properties can be explained on the base of percolation of rigidity theory. The presented method show the potential for fabrication of low-*k* dielectric films for further microelectronic technology nodes.

[1]K. Maex, M. R. Baklanov, D. Shamiryan, F. Iacopi, S. H. Brongersma, and Z. S. Yanovitskaya, J. Appl. Phys. **93**, 8793 (2003).
[2]D. Shamiryan, T. Abell, F. Iacopi, and K. Maex, Mater. Today **7**, 34 (2004).
[3]M. R. Baklanov and K. Maex, Philos. Trans. R. Soc. London, Ser. A **364**, 201 (2006).
[4]G. Dubois, R. D. Miller, and W. Volksen, in *Dielectric Films for Advanced Microelectronics*, edited by M. Baklanov, M. Green, and K. Maex (Wiley, New York, 2007), Chap. 2.
[5]H. Y. Fan, C. Hartshorn, T. Buchheit, D. Tallant, R. Assink, R. Simpson, D. J. Kisse, D. J. Lacks, S. Torquato, and C. J. Brinker, Nat. Mater. **6**, 418 (2007).
[6]G. Dubois, T. Magbitang, W. Volksen, E. E. Simonyi, and R. D. Miller, International Interconnect Technology Conference, Burlingame, CA, 6–8 June, 2005.
[7]D. D. Burkey and K. K. Gleason, J. Appl. Phys. **93**, 5143 (2003).
[8]H. Li, Y. B. Lin, T. Y. Tsui, and J. J. Vlassak, J. Mater. Res. **24**, 107 (2009).
[9]A. Grill, in *Dielectric Films for Advanced Microelectronics*, edited by M. Baklanov, M. Green, and K. Maex (Wiley, New York, 2007), Chap. 1.
[10]R. Sreenivasan and K. K. Gleason, Chem. Vap. Deposition **15**, 77 (2009).
[11]A. Grill and V. Patel, Appl. Phys. Lett. **79**, 803 (2001).
[12]F. Iacopi, Y. Travaly, B. Eyckens, C. Waldfried, T. Abell, E. P. Guyer, D. M. Gage, R. H. Dauskardt, T. Sajavaara, K. Houthoofd, P. Grobet, P. Jacobs, and K. Maex, J. Appl. Phys. **99**, 053511 (2006).
[13]M. R. Baklanov and K. P. Mogilnikov, Microelectron. Eng. **64**, 335 (2002).
[14]P. Marsik, A. Urbanowicz, P. Verdonck, K. Ferchichi, D. De Roest, L. Prager, and M. R. Baklanov, in *Proceedings of 25th Advanced Metallization Conference, 2008*, MRS Symposia Proceedings No. XXIV, edited by M. Naik, R. Shaviv, T. Yoda, and K. Ueno (Materials Research Society, Pittsburgh, 2009), pp. 543–549.
[15]A. M. Urbanowicz, D. Shamiryan, P. Marsik, Y. Travaly, A. Jonas, P. Verdonck, K. Vanstreels, A. Ferchichi, D. De Roest, H. Sprey, K. Matshushita, S. Kaneko, N. Tsuji, S. Luo, O. Escorcia, I. L. Berry, C. Waldfried, S. De Gendt, and M. R. Baklanov, in *Improved Low-k Dielectric Properties Using He/H2 Plasma for Resist Removal*, MRS Symposia Proceedings No. XXIV, edited by M. Naik, R. Shaviv, T. Yoda, and K. Ueno (Materials Research Society, Pittsburgh, 2009), pp. 594–598.
[16]A. M. Urbanowicz, K. Vanstreels, D. Shamiryan, S. De Gendt, and M. Baklanov, Electrochem. Solid-State Lett. **12**, H292 (2009).
[17]A. Zenasni, F. Ciaramella, V. Jousseaume, C. Le Cornec, and G. Passemard, J. Electrochem. Soc. **154**, G6 (2007).
[18]P. Marsik, P. Verdonck, D. De Roest, and M. R. Baklanov, Thin Solid Films **518**, 4266 (2010).
[19]M. Ikeda, S. Nakahira, Y. Iba, H. Kitada, N. Nishikawa, M. Miyajima, S. Fukuyama, N. Shimizu, K. Ikeda, T. Ohba, I. Sagiura, K. Suzuki, Y. Nakata, S. Doi, N. Awaji, and E. Yano, IEEE International Interconnect Technology Conference, 2003.
[20]S. Eslava, G. Eymery, P. Marsik, F. Iacopi, C. E. A. Kirschhock, K. Maex, J. A. Martens, and M. R. Baklanov, J. Electrochem. Soc. **155**, G115 (2008).
[21]M. Matsuura, K. Goto, N. Miura, J. M. Haag, S. Hashii, and K. Asai, in *Film Characterization of Ultra Low-k Dielectrics Modified by UV Curing with Different Wavelength Bands*, MRS Symposia Proceedings No. 914 edited by T. T. Tsui, Y.-C. Joo, L. Michaelson, M. Lane, and A. A. Volinsky (Materials Research Society, Pittsburgh, 2006), p. F01.
[22]G. Aksenov, D. De Roest, P. Verdonck, F. N. Dultsev, P. Marsik, D. Shamiryan, H. Arai, N. Takamure, and M. Baklanov, in *Optimization of*

Low-k UV curing: Effect of Wavelength On Critical Properties of the Dielectric, MRS Symposia Proceedings No. 1156 edited by M. Gall, F. Iacopi, M. Koike, and T. Usui (Materials Research Society, Pittsburgh, 2009), p. D02.
[23]W. Volksen, D. M. Miller, and G. Dubois, Chem. Rev. **110**, 56 (2010).
[24]T. Owada, N. Ohara, H. Watatani, T. Kouno, H. Kudo, H. Ochimizu, T. Sakaoda, N. Asami, Y. Ohkura, S. Fukuyama, A. Tsukune, M. Nakaishi, T. Nakamura, Y. Nara, and M. Kase, "Advanced BEOL Integration Using Porous Low-k (k=2.25) Material With Charge Damage-less Electron Beam Cure Technique," 2009.
[25]I. L. Berry, Q. Han, C. Waldfried, O. Escorcia, and A. Becknell, *SEMI® Technical Symposium: Innovations in Semiconductor Manufacturing*, 2004.
[26]W. Chen, Q. Y. Han, R. Most, C. Waldfried, O. Escorcia, and I. Berry, J. Electrochem. Soc. **151**, F182 (2004).
[27]K. J. Miller, J. Am. Chem. Soc. **112**, 8533 (1990).
[28]D. J. Morris and R. F. Cook, J. Mater. Res. **23**, 2443 (2008).
[29]M. Gonzalez, K. Vanstreels, and A. M. Urbanowicz, 10th International Conference Thermal, Mechanical, and Multiphysic Simulation and Experiments in Micro-Electronic—EuroSimE, Delf, Netherlands, 27 May, 2009.
[30]K. Vanstreels and A. M. Urbanowicz, J. Vac. Sci. Technol. B **28**, 173 (2010).
[31]A. M. Urbanowicz, B. Meshman, D. Schneider, and M. R. Baklanov, Phys. Status Solidi A **205**, 829 (2008).
[32]S. Eslava, F. Iacopi, A. M. Urbanowicz, C. E. A. Kirschhock, K. Maex, J. A. Martens, and M. R. Baklanova, J. Electrochem. Soc. **155**, G231 (2008).
[33]P. Verdonck, D. De Roest, S. Kaneko, R. Caluwaerts, N. Tsuji, K. Matsushita, N. Kemeling, Y. Travaly, H. Sprey, M. Schaekers, and G. Beyer, Surf. Coat. Technol. **201**, 9264 (2007).
[34]J. C. Phillips, J. Non-Cryst. Solids **34**, 153 (1979).
[35]M. F. Thorpe, J. Non-Cryst. Solids **57**, 355 (1983).
[36]G. H. Dohler, R. Dandoloff, and H. Biltz, J. Non-Cryst. Solids **42**, 271 (1980).
[37]R. Anderson, L. L. Larson, and C. Smith, *Silicone Compounds: Register and Review* (Huls America, Bristol, Pennsylvania, 1987).